NOTE

Effects of Shear Rate on the Molecular Orientation in Extruded Rods of a Thermotropic Liquid Crystalline Polymer

INTRODUCTION

The oriented morphologies are developed in the fabrics of liquid crystalline polymers (LCP), because the semirigid molecular chains of LCP follow the flow direction in the processing. It is further pointed out that the complex flow in the processing gives rise to a skin–core structure consisting of highly oriented skin and poorly oriented core.[1-5] The skin–core structure has been observed with scanning electron microscopy and optical microscopy.[1-5] In addition, the orientation distribution in the fabrics of LCP has been analyzed using wide angle X-ray diffraction,[1,6,7] birefringence,[5] and polarized Fourier transform infrared (FTIR) microspectroscopy.[8,9] The orientation in the surface layer of polymeric materials has been probed by the polarized attenuated total reflection (ATR)-FTIR spectroscopy[10-14] and specular reflection spectroscopy.[14,15] We have discussed the effects of draw-down ratio on the orientation distribution of the extruded LCP materials.[8,9,14,15]

In this work, the orientation distribution in extruded rods of a thermotropic liquid crystalline copolyester is studied with polarized FTIR microspectroscopy and polarized ATR-FTIR spectroscopy. Particular attention is focused on the effect of shear rate on the orientation distribution in the LCP rods.

EXPERIMENTAL

The sample studied in this work is a thermotropic liquid crystalline copolyester consisting of 73 mol % of 4-hydroxybenzoic acid units and 27 mol % of 2-hydroxy-6-naphthoic acid units. Prior to the extrusion, the pellets (Polyplastic Co., Ltd.) of the copolyester were dried at 90°C for 12 h and at 120°C for 3 h. The LCP rods were extruded into a cooling bath using a twin-screw extruder equipped with a circular tube die. The sketch of the extruder is shown in Figure 1. The length of the circular tube region was 40 mm, and the diameter of the die orifice was 2 mm. The entrance region of the die was conically designed. The die temperature was controlled at 310°C. The shear history by the twin-screw rotations was expected to be reduced during the slow flow in the crosshead region with a diameter of 14 mm. The post elongation of extruded material was restricted as much as possible, and draw-down ratio was controlled to lie in the range of 1.0–1.2. The apparent shear rate was controlled by changing the mass output. The value of apparent shear rate, $\dot{\gamma}_a$, was calculated from volumetric flow (Q), density (d), mass output (M), and the diameter of die (D).[16]

$$\dot{\gamma}_a = 32Q/(\pi D^3) = 32M/(\pi d D^3) \quad (1)$$

The extruded rods were microtomed in the extrusion direction to a thickness of 10 μm after the rods were embedded in an epoxy resin. The microtomed sections were characterized by polarized FTIR microspectroscopy. The polarized FTIR microspectra were measured on a Perkin–Elmer Model 1800 FTIR spectrometer equipped with a liquid-nitrogen-cooled MCT detector. The 500 scans of 4 cm^{-1} resolution were averaged so as to obtain a sufficient signal-to-noise ratio. The microbeam radiation was obtained with a redundantly apertured infrared microscope, IR Plan Model 100 (Spectra-Tec, Inc.). The microbeam with 100 × 200 μm was focused on samples. The polarized spectra were obtained using a wire-grid polarizer.

The specimen for the FTIR microspectroscopy is shown in Figure 2. If the dichroic spectra of the section microtomed from the central part were measured at various positions of the section, the spectra polarized in the extrusion direction (ED) and the radial direction (RD) were obtained (Fig. 2[a]). If the dichroic spectra were measured at the central part of sections which were microtomed from various parts of the strand, the dichroic spectra between the extrusion direction and the tangential direction (TD) were obtained (Fig. 2[b]).

The surface orientation was characterized with polarized ATR-FTIR spectroscopy. It is difficult to measure the ATR–FTIR spectra of thick rods as they are. The preparation of the specimen for ATR–FTIR measurements is shown in Figure 3. The highly oriented skin layer was peeled off the LCP strand and cut into strips 25 mm long. The strips were carefully affixed on the substrate with the extrusion direction parallel to each other.

Polarized ATR-FTIR spectra were measured at a 45° angle of incidence with an FTIR spectrometer equipped with a rotable ATR accessory, liquid-nitrogen-cooled MCT detector, and wire-grid polarizer. The design for the rotable ATR accessory (Harrick Scientific Corp.) was first reported by Sung and her coworkers.[11,13] The ATR crystal used was a double-edged germanium crystal (25 × 25 × 2 mm). The ATR accessory allows us to rotate the sample and the ATR crystal without remounting them.

Journal of Applied Polymer Science, Vol. 55, 1489–1493 (1995)
 CCC 0021-8995/95/101489-05

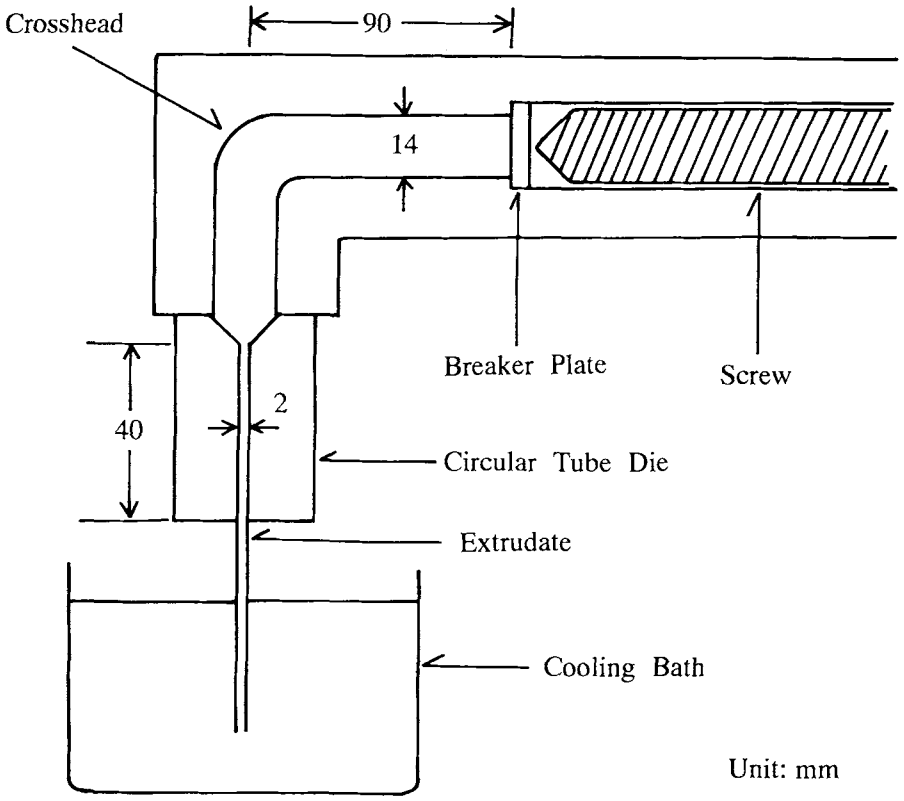

Figure 1 Sketch of the extruder equipped with a circular tube die.

RESULTS AND DISCUSSION

The LCP rods were extruded in the apparent shear rate range of 20–800 sec^{-1}. The appearance of the extruded strand strongly depends upon apparent shear rate. If the apparent shear rate is less than 150 sec^{-1}, the LCP rods contain many voids and have rough surfaces. It is difficult to characterize the samples extruded at low apparent shear rate because of high void content. With increasing apparent shear rate, however, the surface becomes smooth and the void fraction decreases.

The polarized FTIR spectra were measured in a microscopic area of 100 × 200 μm, at various positions from the center to the surface. The orientation function in the microscopic area can be determined by the polarized FTIR microspectra. The orientation profiles are obtained by plotting the microscopic orientation function against the distance from the center of rods. The microscopic orientation function, f_i, is calculated from the dichroic ratio ($A_{i//}/A_{i\perp}$) of the i-th absorption bands.

$$R_i = A_{i//}/A_{i\perp} \tag{2}$$

$$f_i = (R_i - 1)/(R_i + 2) \tag{3}$$

The orientation function of f_i represents the orientation of the transition moment of the ith absorption band. If the angle ω_i between the transition moment and the polymer chain axis is known, the orientation function f of the polymer chain can be determined.

$$f = 2f_i/(3\cos^2\omega_i - 1) \tag{4}$$

In this work, the microscopic orientation function was calculated from the dichroic ratio of the 1474 cm^{-1} band

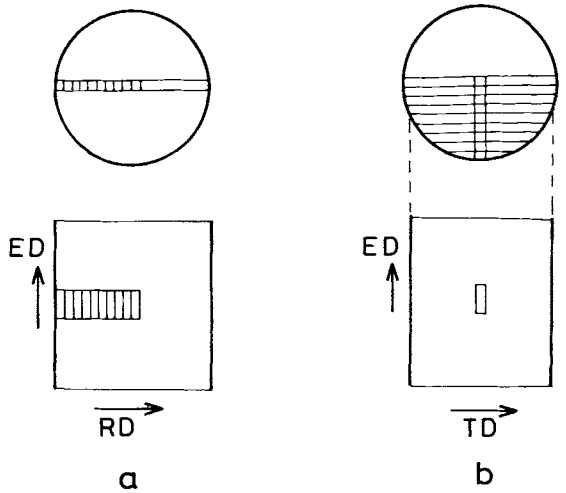

Figure 2 Microtomed section of an LCP rod used for the measurements of FTIR microspectroscopy.

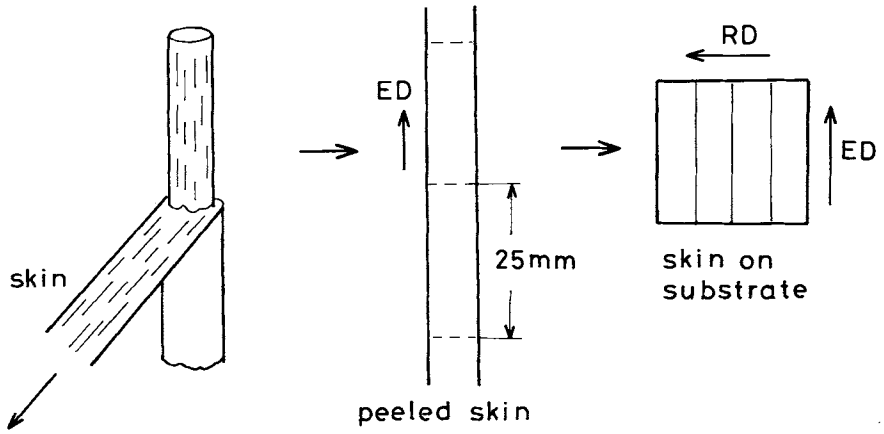

Figure 3 Sample preparation for the measurements of polarized ATR-FTIR spectra.

which is assigned to the CC stretching vibration of the naphthalene ring. This band gives the highest dichroic ratio among the bands in the region of 1350–1650 cm^{-1}, and its transition moment angle, ω_{1474}, was evaluated to be 0–19.5°.[15]

The radial distributions of orientation functions are shown in Figures 4–6. The circles stand for the orientation function calculated from the absorbance in the extrusion direction and the radial direction ($f_{ED/RD}$). The triangles represent that obtained from the absorbance in the extrusion direction and the tangential direction ($f_{ED/TD}$). In the central region of the extruded rods, the orientation function lies in the range of 0.0–0.05, and the central regions of the LCP rods are nearly isotropic regardless of the apparent shear rate. The orientation function, however, markedly increases with the change of position from the center to the surface. The values of $f_{ED/RD}$ tend to be higher than those of $f_{ED/TD}$ in the region of distance/diameter = 0.1–0.4, suggesting that the fraction of molecular chains orienting to RD is less than that orienting to TD. On the other hand, the orientation function in the surface region is affected by apparent shear rate. The orientation function in the surface region increases with increasing apparent shear rate from 166 to 506 sec^{-1}, but the orien-

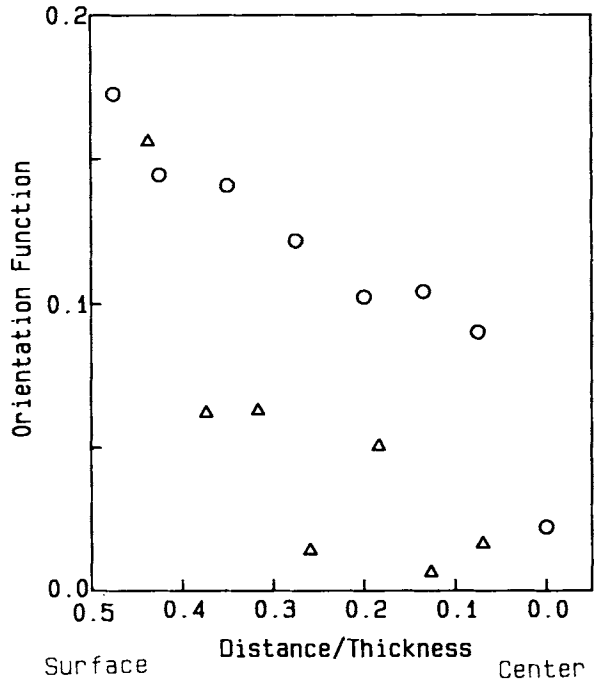

Figure 4 Orientation profiles of the LCP rod extruded at $\dot{\gamma}_a$ = 166 sec^{-1}: (○) $f_{ED/RD}$; (△) $f_{ED/TD}$.

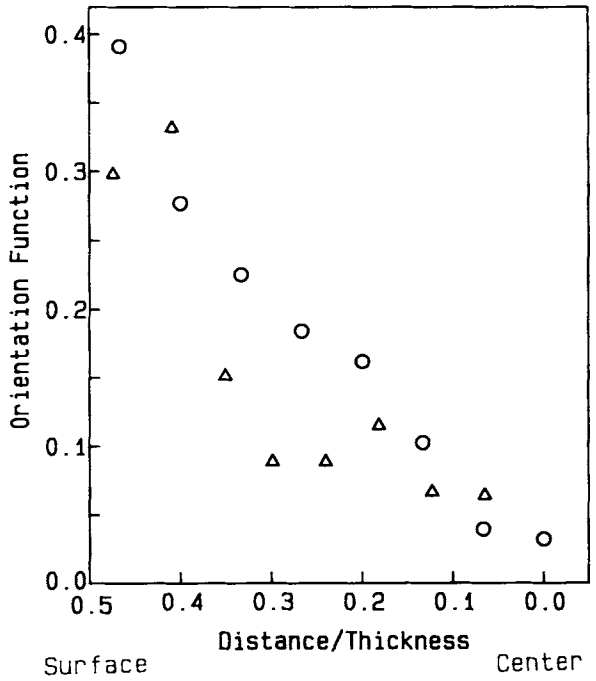

Figure 5 Orientation profiles of the LCP rod extruded at $\dot{\gamma}_a$ = 506 sec^{-1}: (○) $f_{ED/RD}$; (△) $f_{ED/TD}$.

tation function decreases with further increasing apparent shear rate to 776 sec^{-1}.

The polarized ATR-FTIR spectra are shown in Figure 7. The electric vector for the transverse magnetic (TM) wave lies in the plane of incidence, while that for the transverse electric (TE) wave is perpendicular to the plane of incidence. A(TE1) and A(TM1) are the absorbance for TE wave and TM wave, respectively, measured with extrusion direction normal to the plane of incidence. The absorbance, A(TE2), is obtained using the TE wave with transverse direction normal to the plane of incidence. The absorbances, A(TE1), A(TE2), and A(TM1), are related to the three-dimensional absorbances, A_{ED}, A_{RD}, and A_{TD}.[10]

$$A(\text{TE1}) = \alpha A_{ED} \tag{5}$$

$$A(\text{TE2}) = \alpha A_{RD} \tag{6}$$

$$A(\text{TM1}) = \beta A_{RD} + \gamma A_{TD} \tag{7}$$

where α, β, and γ are functions of angle of incidence and refractive indices of samples and the ATR crystal. The absorbance in the spectra A(TE1) is much higher than that in the spectra A(TE2) and A(TM1) for many absorption bands in the wavenumber region of 900–1650 cm^{-1}. The relative band intensities in the spectra A(TE2) are similar to those in A(TM1). The results show that the molecular chains are oriented uniaxially in the extrusion direction, and that the surface orientation in the radial direction is nearly equivalent to the orientation in the tangential direction.

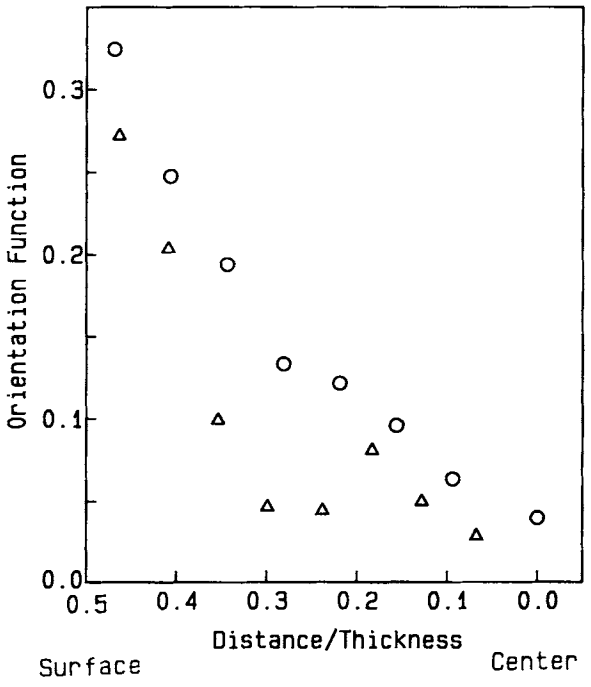

Figure 6 Orientation profiles of the LCP rod extruded at $\dot{\gamma}_a$ = 776 sec^{-1}: (○) $f_{ED/RD}$; (△) $f_{ED/TD}$.

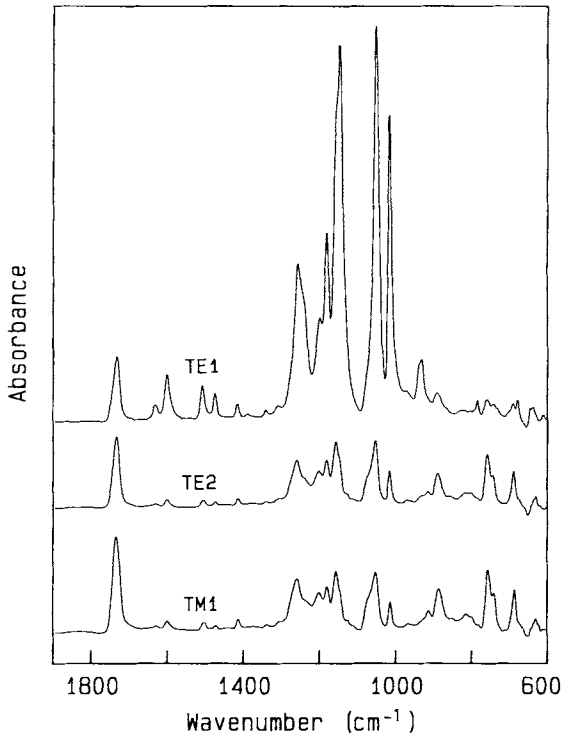

Figure 7 Polarized ATR spectra of the LCP rod extruded at $\dot{\gamma}_a$ = 506 sec^{-1}.

The surface orientation functions were calculated for the 1601, 1506, 1473, and 1010 cm^{-1} bands from the absorbances A(TE1) and A(TE2).

$$R_i = A_i(\text{TE1})/A_i(\text{TE2}) = A_{ED}/A_{RD} \tag{8}$$

$$f_i = (R_i - 1)/(R_i + 2) \tag{9}$$

The results are shown in Figure 8 as a function of the apparent shear rate. The values of orientation functions depend upon the absorption bands because they are affected by the transition moment angle of the molecular vibration. The depth probed by the ATR-FTIR spectroscopy depends upon the angle of incidence and refractive indices of sample and the ATR crystal (n_s and n_c, respectively). If ATR-FTIR spectrum is measured at a 45° angle of incidence using a germanium ATR crystal (n_c = 4.0), the depth is calculated to be 0.5 μm at 1500 cm^{-1}. Thus the polarized ATR-FTIR spectroscopy measures the orientation function of the thin surface layer, which cannot be probed by the polarized FTIR microspectra. The surface orientation function determined by polarized ATR-FTIR spectra is much higher than the microscopic orientation function obtained by polarized FTIR microspectra. The result shows that the orientation function increases on approaching the surface, and that the increase of orientation is marked near the surface.

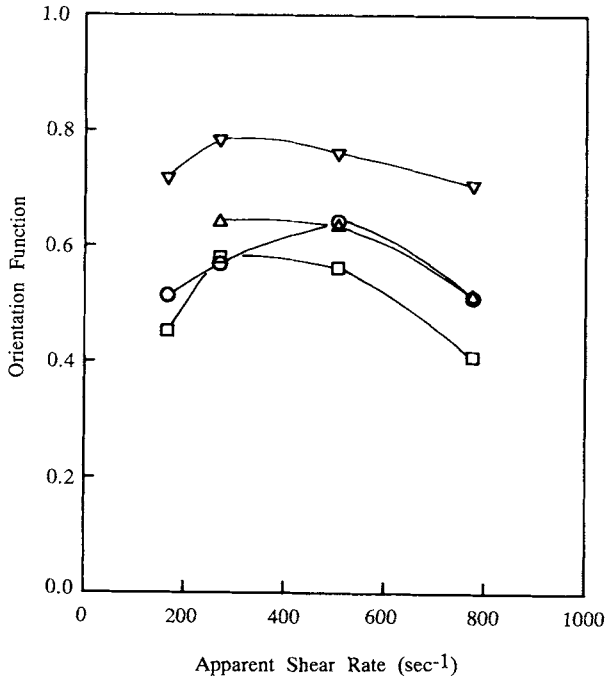

Figure 8 Surface orientation function of LCP rod as a function of apparent shear rate: (○) 1601 cm^{-1}; (□) 1506 cm^{-1}; (△) 1473 cm^{-1}; (▽) 1010 cm^{-1}.

The orientation function increases with increasing apparent shear rate from 166 to 270 sec^{-1}, but decreases with increasing apparent shear rate from 506 to 780 sec^{-1}. The results obtained by polarized ATR-FTIR spectroscopy are consistent with those of polarized FTIR microspectroscopy. The reason for the decrease of surface orientation function in the apparent shear rate range of 506–780 sec^{-1} is not clearly explained. One possible explanation is that the polymer melt stays in the die for a shorter time with increasing extrusion rate, and the orientation function decreases with increasing extrusion rate.

REFERENCES

1. K. Shimamura, J. L. White, and J. F. Feller, *J. Appl. Polym. Sci.*, **26,** 2165 (1981).
2. Y. Ide and Z. Ophir, *Polym. Eng. Sci.*, **23,** 261 (1983).
3. L. C. Sawyer and M. Jaffe, *J. Mater. Sci.*, **21,** 1897 (1986).
4. T. Weng, A. Hiltner, and E. Baer, *J. Mater. Sci.*, **21,** 744 (1986).
5. Y. Takeuchi, Y. Shuto, and F. Yamamoto, *Polymer,* **29,** 605 (1988).
6. K. Itoyama and T. Yamakawa, *Kobunshi Ronbunshu,* **45,** 925 (1988).
7. D. J. Blundell, R. A. Chivers, A. D. Curson, J. C. Love, and W. A. MacDonald, *Polymer,* **29,** 1459 (1988).
8. A. Kaito, M. Kyotani, and K. Nakayama, *Macromolecules,* **24,** 3244 (1991).
9. A. Kaito, M. Kyotani, and K. Nakayama, *Polymer,* **33,** 2672 (1992).
10. P. A. Flournoy and W. A. Schaffers, *Spectrochim Acta,* **22,** 5 (1966).
11. C. S. P. Sung, *Macromolecules,* **14,** 591 (1981).
12. F. M. Mirabella, Jr., *J. Polym. Sci., Polym. Phys. Ed.,* **22,** 1283, 1293 (1984).
13. A. Pirnia and C. S. P. Sung, *Macromolecules,* **21,** 2699 (1988).
14. A. Kaito and K. Nakayama, *Macromolecules,* **25,** 4882 (1992).
15. A. Kaito, K. Nakayama, and M. Kyotani, *J. Polym. Sci., Polym. Phys. Ed.,* **29,** 1321 (1991).
16. C. D. Han, *Rheology in Polymer Processing,* Academic Press, New York, 1976, p. 105.

A. KAITO*
M. KYOTANI
K. NAKAYAMA
National Institute of Materials and Chemical Research
1-1, Higashi, Tsukuba
Ibaraki 305, Japan

Received April 12, 1994
Accepted August 8, 1994

* To whom correspondence should be addressed.